

4.1.A Appendix: Beamline Sensitivity Effects

The sensitivity of the beamline to various off-nominal conditions has been investigated. Specifically addressed are the sensitivities of focus and of trajectory.

Focusing sensitivity The sensitivity of the optics to different error sources has been studied in simulations. Assigning random gradient errors of $\sigma(\Delta B'/B') = 25 \times 10^{-4}$ to the 21 quadrupoles in the line, **Figure 4.1.A-1** shows the beam sizes resulting from 20 random generator seeds. The changes in beam σ 's are demonstrated to be less than ≈ 0.1 mm. At the target the maximum changes in beam size are on the order of 0.05 mm, within the specification.

Optical errors also arise from discrepancies between the assumed and actual MI lattice functions. **Figure 4.1.A-2** shows the β -envelopes (proportional to squares of beam sizes) that result from $\pm 10\%$ variations in the nominal β_x and β_y values. The maximum β 's are sufficiently well-behaved that no aperture problems arise, and the small residual mismatch at the target can be corrected with 4 or 6 final-focus quadrupoles.

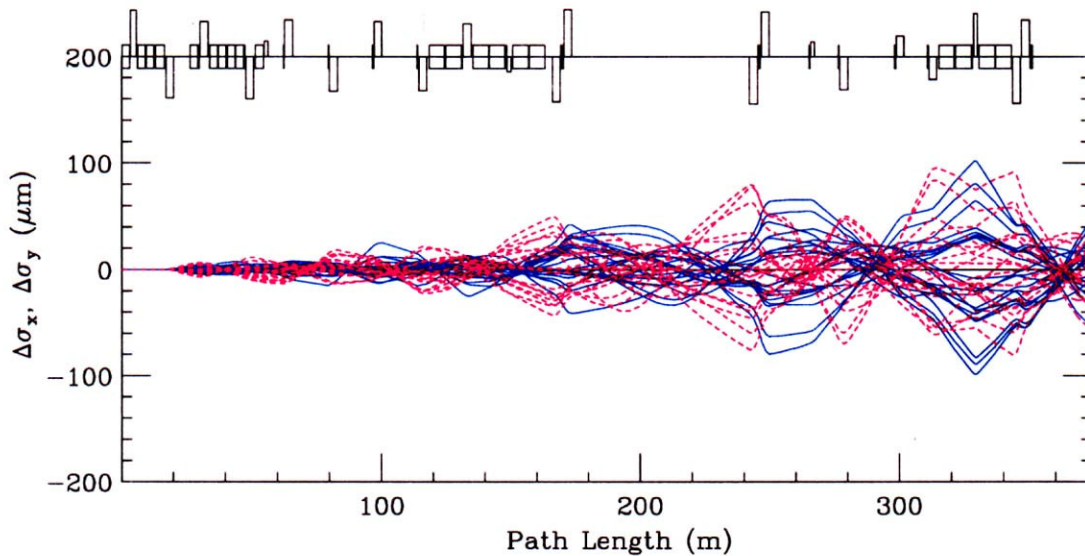


Figure 4.1.A-1. Beam size variation resulting from random gradient errors

Trajectory sensitivity and correction Most focusing elements in the line have associated position monitors. Orbit correction is an issue which, of course, must be addressed by any beamline, but for the ultra-clean transport requirements of NuMI it is critical that precise position control be available throughout.

Correction of central trajectory errors has been simulated with dipole field errors and random misalignments assigned to the beamline elements (including position monitors). Suitable error values are 0.25 mm for positions and 10^{-3} for magnetic field fractions. Figure A3 shows the deviations from the central trajectory arising from 20 random error seeds. The uncorrected

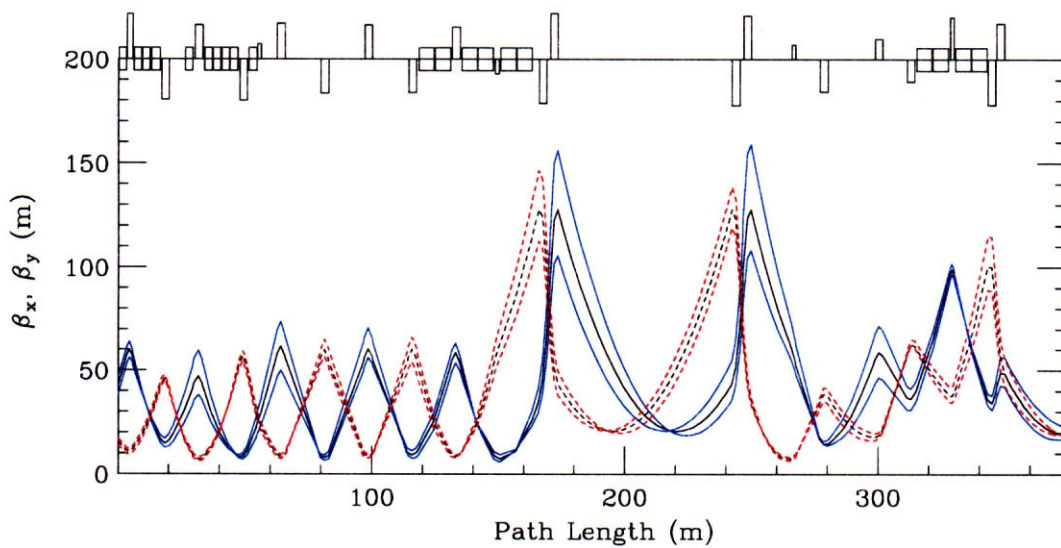


Figure 4.1.A-2. β -waves due to $\pm 10\%$ injection optic errors

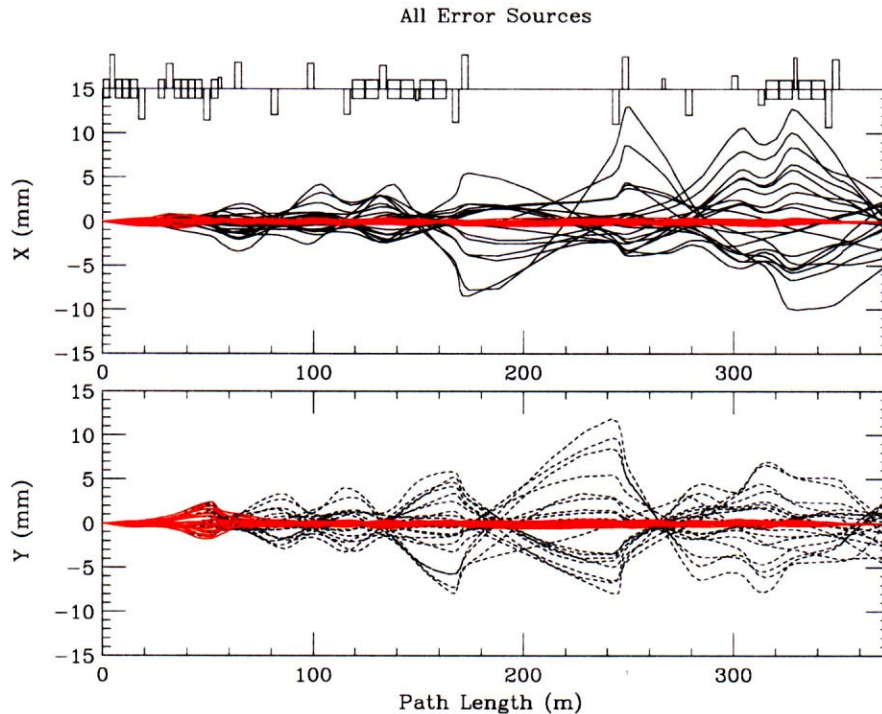


Figure 4.1.A-3. Uncorrected and corrected trajectories with random misalignments and dipole field errors

offsets in the line are $\Delta x(\text{rms}) = 2.63$ mm, $\Delta x(\text{max}) = 13.03$ mm, and $\Delta y(\text{rms}) = 2.33$ mm, $\Delta y(\text{max}) = 11.90$ mm. There is some concern, however, that the NuMI positioning errors will be greater than .25 mm, at least originally, in which case the trajectory errors will scale accordingly.

The orbits from the above analysis as corrected by the trim magnets are shown in red in the figure. They are, again, within specification, though for the vertical they require more trim strength than is available in MI vertical correctors. It is for this reason that rolled horizontal correctors are specified for the vertical plane.

The sensitivity of the line to possible dipole mispowering is a subject of considerable interest and is now presented in greater detail. **Figure 4.1.A-4a** shows the situation for the horizontal plane and **Figure 4.1.A-4b** for the vertical. What is plotted is, for each bend supply, the effect on downstream beam positions of a .1% power supply drift of the peak current. Comparing with the specification of <0.5 mm for target position (the target is located at station 356 meters), it is seen

that at least the major up and down bends will need regulation considerably greater than that used in making the figure. Taking into account the specification for stability along the beamline, the EPB string also requires more regulation. The power supply stability specifications resulting from this analysis are presented in the Section 4.3 of this Handbook. They are accomplished via techniques in use elsewhere in the laboratory.

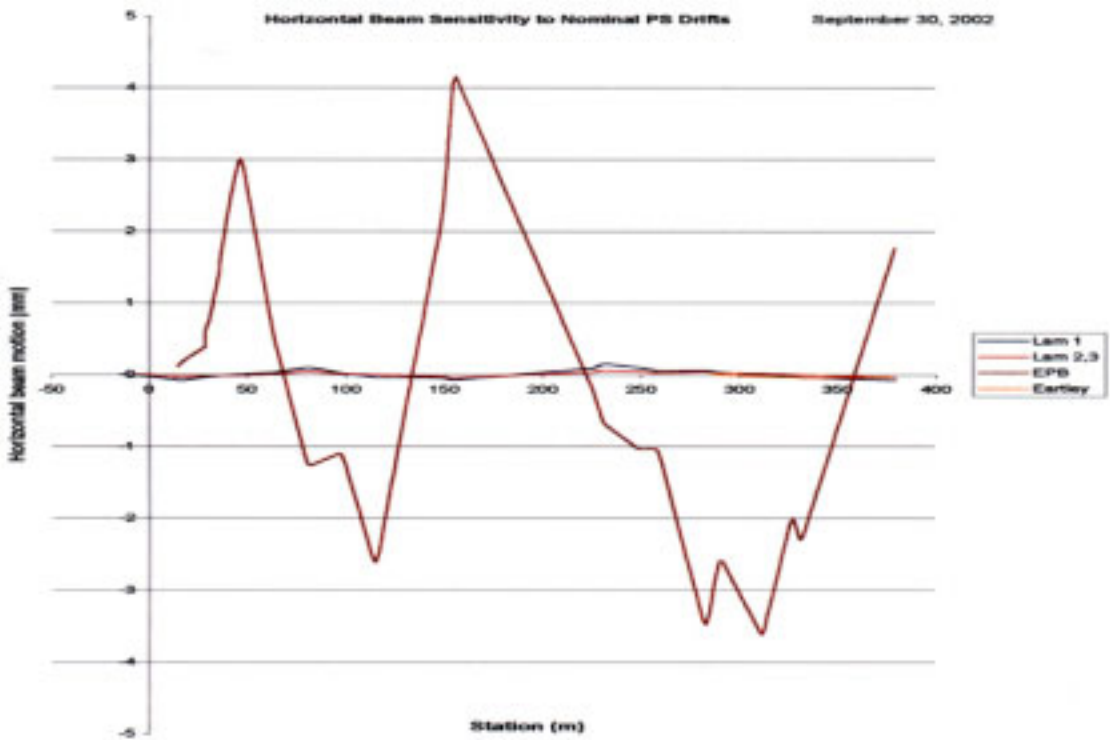


Figure 4.1.A-4a. Sensitivity in the horizontal plane to dipole power supply variations

Vertical Beam Sensivity to Nominal PS Drifts

September 30, 2002

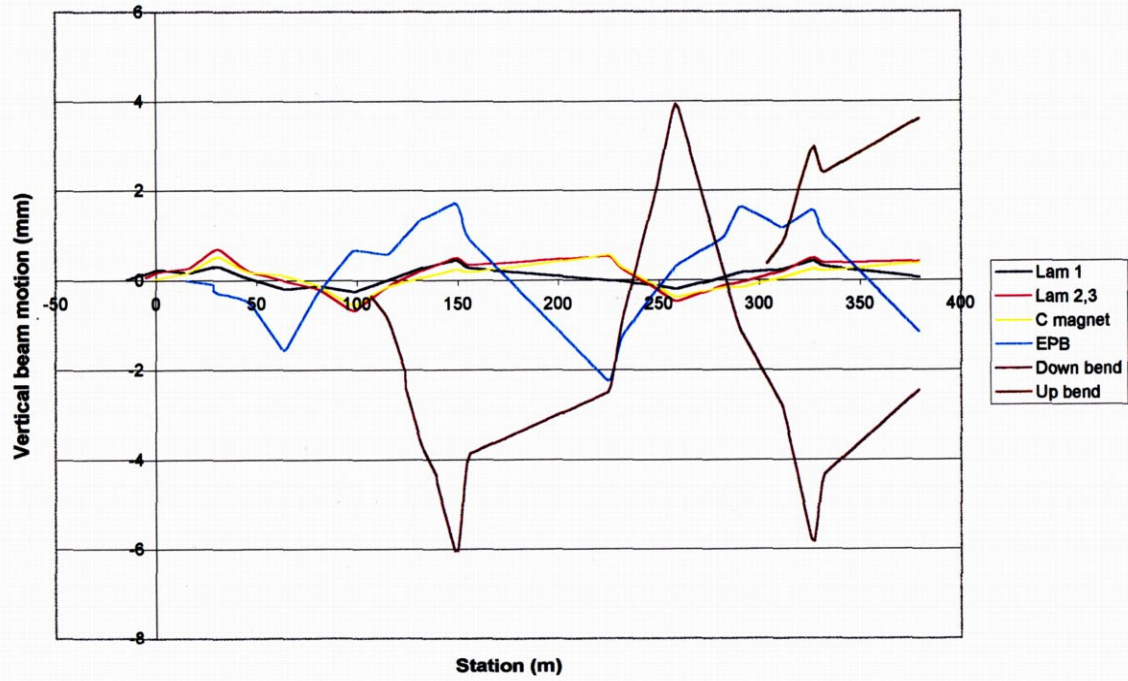


Figure 4.1.A-4b. Sensitivity in the vertical plane to dipole power supply variations

4.1.B Appendix : Aperture Considerations

Figure 4.1.B-1 shows the amplitude (root β) and dispersion (η) functions over the entire line. The beam size peaks at stations 150 m and 225 m are at the upstream and downstream ends of the unoccupied carrier region. Putting relatively large sizes at these quadrupoles allows the sizes upstream and downstream of them to be appropriately small. To prevent the running of any quadrupole at a current value that would endanger it, a limit of 16.0 T/m has been placed on the gradients.

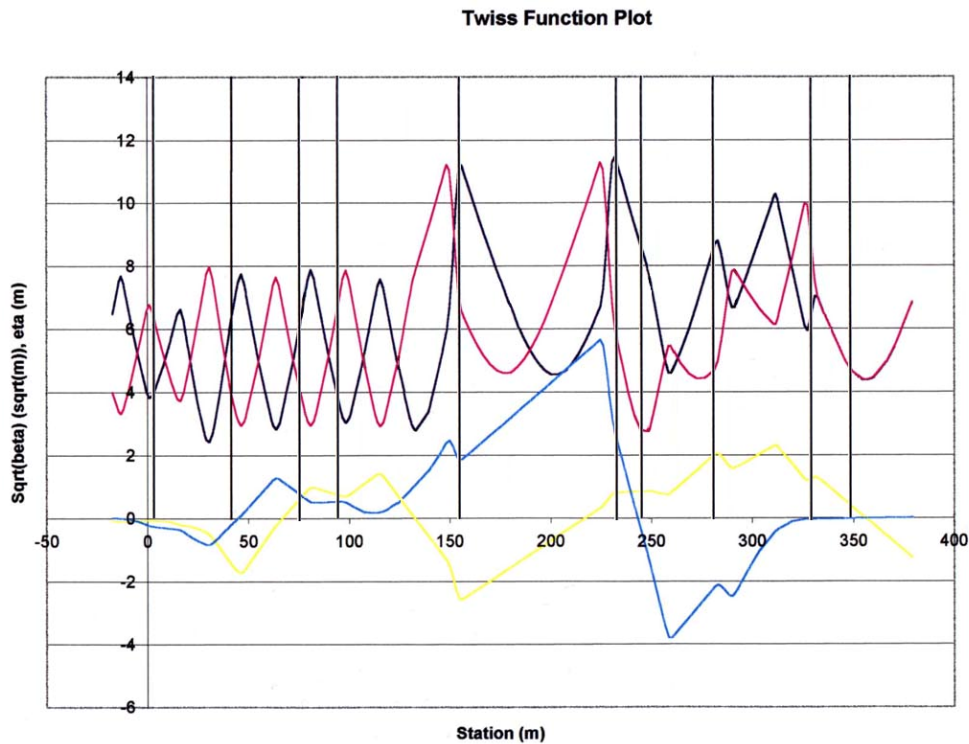


Figure 4.1.B-1. Amplitude and dispersion plots over the entire beamline. The target station value is 356 meters. The vertical lines indicate the locations of the 10 multiwire profile monitors.

Figure 4.1.B-2a shows the clearances vs. beam size over the entire line and **Figure 4.1.B-2b** shows an expanded view of the same in the Lambertson region. Considerable effort has gone into having a design for which this plot demonstrates adequate clearance over the length of the entire beamline, and several of the plot's features are worthy of detailed discussion. The aperture, or preferably clearance, shown for each element is the actual half-aperture of the device minus any sagitta in that device.

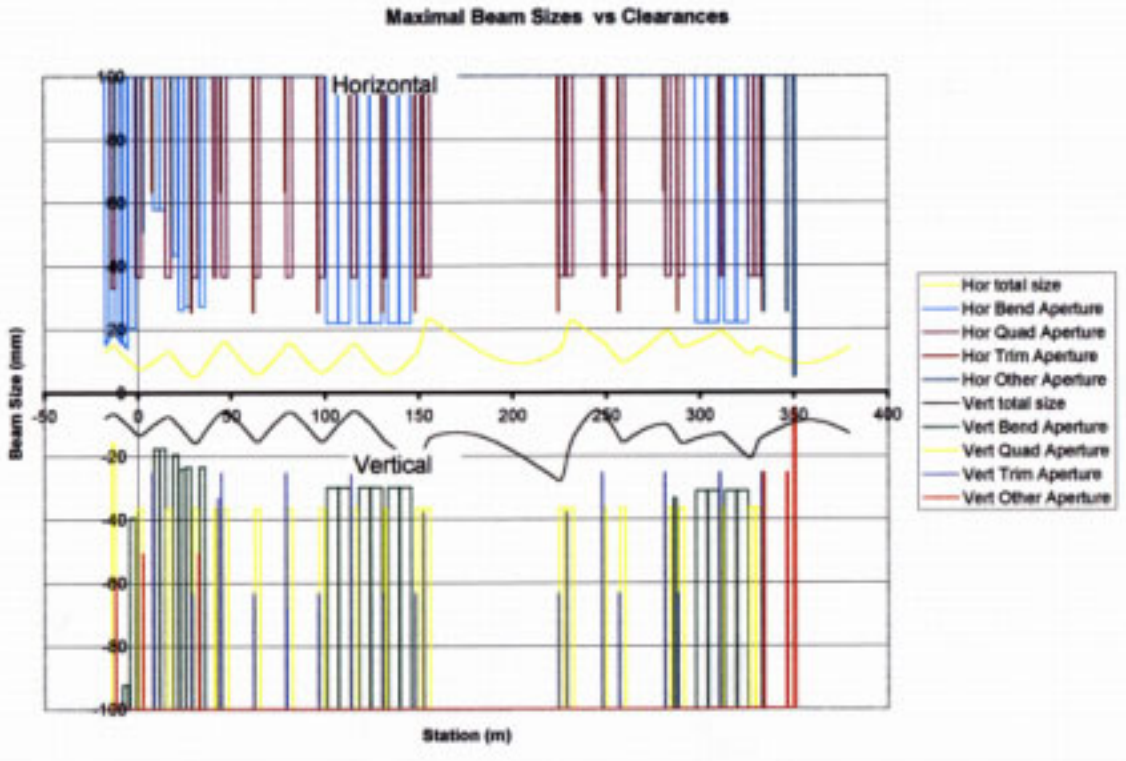


Figure 4.1.B-2a. Beam and aperture clearance plot over the entire beamline

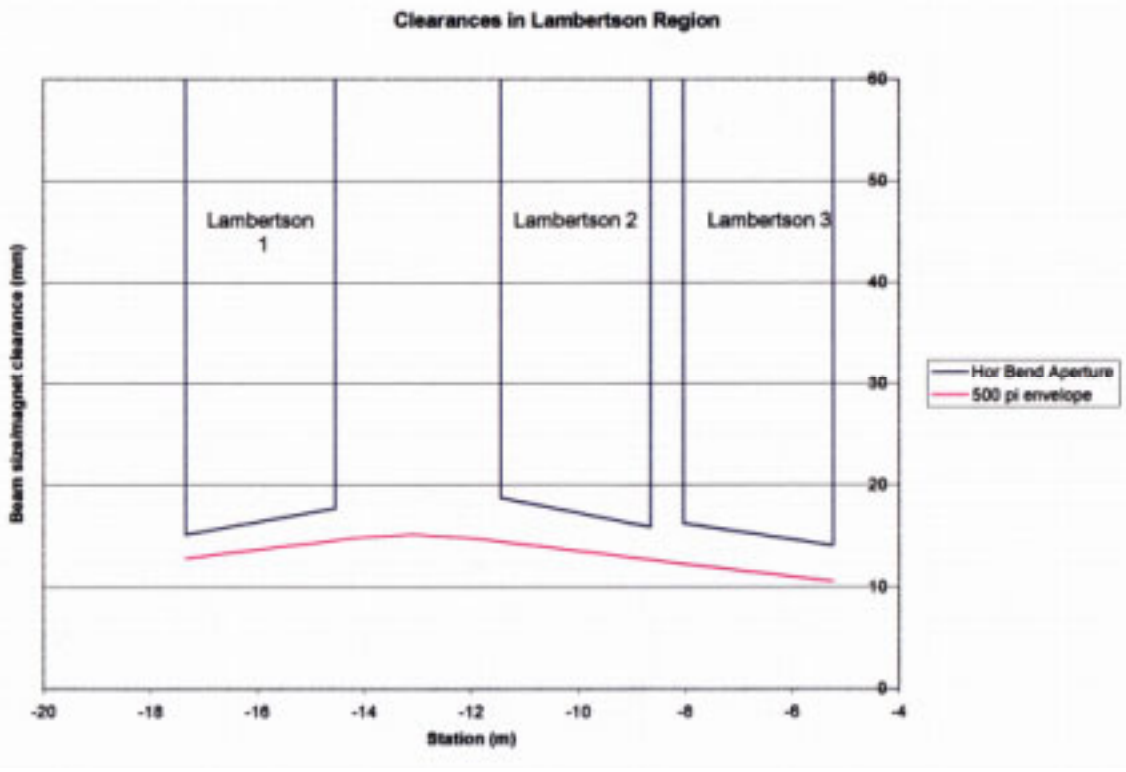


Figure 4.1.B-2b. Beam and aperture clearance plot in extraction region

However what is shown as clearance for the Lambertsons, and for MI quadrupole 608 which lies between Lambertsons 1 and 2, is worthy of special comment. The alignment of each of these magnets is determined by the path of the circulating MI beam, not the extracted beam. Thus the effective clearance is the distance from the beam center to the nearest aperture restriction, which for all Lambertsons is the septum. Note that the tighter clearance is in the horizontal plane and that the first two Lambertsons are rolled so that the horizontal distance to the septum is dependent on the height of the beam. Secondly, since the magnets are aligned along the circulating beam direction, the extracted beam is not traveling parallel to the septum face. Additionally, the beam size can change over the length of one element, again affecting the effective clearance. All of these effects have been accounted for in making the plots, which have what appears as angled magnet apertures but which really are angled beam trajectories. Similarly for the case of Q608, what are plotted as clearances are horizontal and vertical distances to the edge of a star shaped vacuum chamber.

As to the beam size plotted, what is shown corresponds to the MI *admittance*, i.e. the largest beam size that the accelerator could possibly spew forth. The figure indicates that the beamline can indeed transmit this worst possible beam. Note also that the desired criteria at the target are met – the beam size has a minimum in both planes at that location.

At station 350 m is an aperture through which the beam apparently does not fit. This aperture is that of the horn protection baffle. The worst case beam, as is plotted here, will indeed not fit through this baffle. However the more nominal beam size, as is expected in general, does fit.